ISBN: 978-3-95450-247-9 ISSN: 2673-5490 doi: 10.18429/JACoW-IPAC2024-THPC15

# TAIL POPULATION STUDIES IN THE CERN PROTON SYNCHROTRON (PS)

M. Bozatzis*[,1], F. Asvesta, H. Bartosik, A. Huschauer, A. Lasheen, E. Maclean, T. Prebibaj, W. Van Goethem, CERN, Geneva, Switzerland
[1]also at Aristotle University of Thessaloniki, Thessaloniki, Greece

*Abstract*

The beam quality in terms of the transverse beam profiles from the CERN injectors plays a crucial role for the luminosity production at the LHC. Transverse tails beyond a Gaussian distribution have been observed in all the LHC injectors and efforts to optimize them are ongoing, as they can perturb operations due to large losses at LHC injection. At the CERN Proton Synchrotron (PS), measurements with various beam parameters and at different points along the cycle have been conducted to identify the source of the additional tails' population. Transition crossing was identified as the most critical point in the shaping of the profiles. Consequently, measurements of the optics perturbations during the $\gamma_t$-jump have been conducted. Simulations of the full transition crossing process including space charge effects have also been performed to fully characterize the effects.

## INTRODUCTION

Transverse beam profile measurements have shown that non-Gaussian tails are developed at various stages of the beam propagation along the LHC injector complex [1]. These particle distribution profiles with overpopulated tails can be characterise using q-Gaussian distributions, as previously applied to measured profiles from the LHC [2] and the Proton Synchrotron Booster (PSB) [3].

The PS has been identified as the accelerator of the injector chain that contributes the most to the tail generation along the complex [1], in particular the transition crossing process. The LHC beams are injected in the PS at 2 GeV and accelerated to 26 GeV. The transition energy of the PS is at $\gamma_t \approx 6.1$ and so transition needs to be crossed in routine operation. To minimize adverse effect from beam instabilities during transition crossing, a $\gamma_t$-jump scheme was implemented [4]. In this work, the effect of the $\gamma_t$-jump scheme on the optics and the transveres beam profiles was studied through measurements and simulations.

## TRANSVERSE TAILS AT THE CERN PS

Gaussian distributions are insufficient for describing the beam characteristics in the presence of overpopulated tails in the transverse profiles. Instead, q-Gaussian distributions are adequate in most of these cases. The parameter $q$ of this distribution describes the significance of the tails. When $q < 1$, the tails are underpopulated compared to a normal Gaussian, when $q = 1$, the q-Gaussian reduces to a normal Gaussian distribution, while for $q > 1$ overpopulated tails are observed. Larger values of the $q$ factor represent more significant tail populations.

In order to characterise the transverse beam profiles, a series of measurements were performed in the CERN PS. The emittance and the q-factor, extracted from the Gaussian and the q-Gaussian fit of the profiles respectively, are used to monitor the beam behaviour in the transverse planes all along the PS cycle and with different beam intensities injected.

### *Tail Population Along the Cycle*

The PS cycle for the operational LHC type beams is shown in Fig. 1. It accommodates two injections from the PSB at an energy of 2 GeV, first four bunches at 170 ms and then two bunches at 1370 ms cycle time. During the intermediate energy plateau (1500 ms – 1900 ms), longitudinal triple splitting is applied to form 18 bunches. During acceleration the beam crosses transition energy at ≈2030 ms and finally reaches the top energy of 26 GeV. Before the protons are extracted to the Super Proton Synchrotron (SPS), two double splittings are applied to create the final train structure of 72 bunches of the standard LHC beam [5].

Transverse profiles were measured with the wire scanners [6] after each significant event of the cycle described above. Since the horizontal profiles are affected by the momentum spread of the beam in combination with the horizontal dispersion [7], $D_x \approx 2.3$m in the location of the horizontal wire scanner, only the vertical plane is considered here. The results are summarized in Fig. 1.

The normalized vertical emittance stays relatively constant along the cycle with small fluctuations of 9%. It should

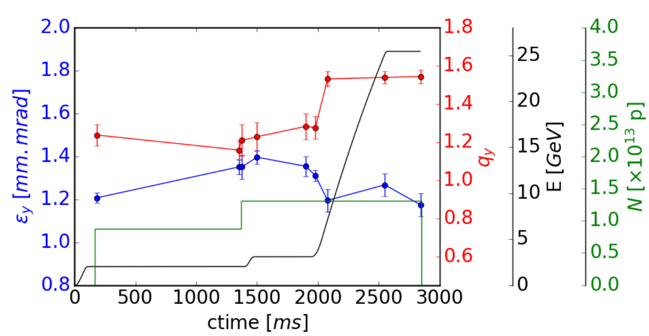


Figure 1: Vertical emittance (blue) and q-factor (red, secondary axis) along the PS cycle for the LHC type beam with 72 bunches at extraction with an intensity of $1.81 \times 10^{11}$ ppb. The proton energy (black, secondary axis) and the timing of the two injections from the PSB (green, secondary axis) are also shown.

* miltiadis.bozatzis@cern.ch

ISBN: 978-3-95450-247-9 ISSN: 2673-5490 doi: 10.18429/JACoW-IPAC2024-THPC15



be noted that the variance of a Gaussian and a q-Gaussian fit differs, depending on the tails of the distribution. The emittance values are conventionally calculated using a normal Gaussian fit. On the other hand, a q-Gaussian fit shows that the tail population increases along the cycle as the q-factor goes from 1.24 at injection to 1.54 at extraction. The largest tail population increase seems to be occurring at transition crossing, where the q-factor suffers a 20% increase.

### *Brightness Curve and Tail Generation*

In order to monitor the tail population, the emittance blow-up and the overall brightness behaviour of the PS, a series of transverse profile measurements were performed at the first injection and at extraction, for different beam intensities. The measurements of the horizontal profiles are taken using the newly deployed zero dispersion (at the location of the horizontal wire scanner) optics [8].

The brightness curve at PS extraction is close to the LHC Injectors Upgrade (LIU) target [9], with a maximum deviation of 5% for the high intensity regime, i.e. $N_b \geq 1.5 \times 10^{11}$ ppb, as shown in Fig. 2 (top). In addition, the horizontal emittances at injection were accurately measured for

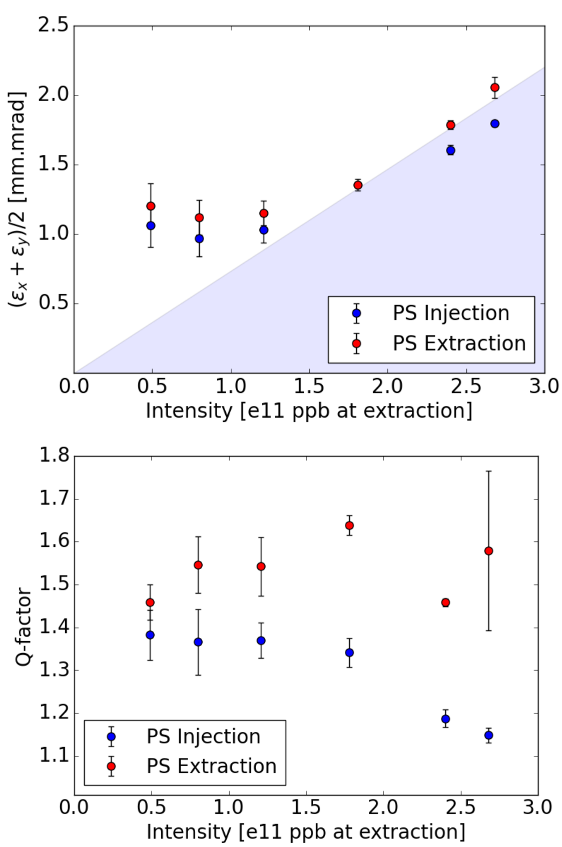


Figure 2: Top: PS brightness curve, i.e. average emittance $\frac{\epsilon_x+\epsilon_y}{2}$ as a function of intensity, at injection with the zero dispersion optics (blue) and at extraction (red). The LIU target is shown by the line delimiting the faded blue area. Bottom: Vertical q-factor at PS injection (blue) and extraction (red) for different intensities.

the first time after the LIU upgrades thanks to the zero dispersion optics. On average, a blow-up of 12% is observed. However, it should be noted that only the Gaussian fit is considered at this stage.

The q values from the corresponding q-Gaussian fits are shown in Fig. 2 (bottom). The q-factor of the vertical profiles at PS injection gets smaller with increasing intensity, meaning that the transverse profiles injected from PSB are more Gaussian. However, the q-factor increase along the PS cycle increases with intensity, indicating a brightness dependent mechanism. This is also demonstrated by the direct comparison of the vertical profile between PS injection and extraction for different intensities, as plotted in Fig. 3. The profiles have been normalized to account for the energy ramp and the consequent beam size reduction.

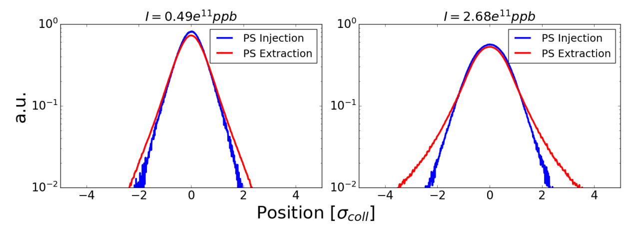


Figure 3: Comparison of injection (blue) and extraction (red) vertical profiles for an intensity of $0.49 \times 10^{11}$ ppb (left) and $2.68 \times 10^{11}$ ppb (right), in logarithmic scale. The $\sigma_{\text{coll}}$ metric represents the profile normalisation convention that corresponds to the standard deviation of a Gaussian profile with an emittance of 3.5 $\mu$m.

## PS OPTICS AT TRANSITION CROSSING

The measurements along the PS cycle showed a significant tail population increase during transition crossing. As mentioned, a $\gamma_t$-jump scheme is needed in order to cross the transition as efficiently as possible to limit any impact on the PS performance [4]. Quadrupoles arranged in doublets and triplets configurations are powered with specific strength functions to adjust the momentum compaction factor $\alpha_p$ and $\gamma_t$. This configuration ensures that the proton energy is far from transition for a longer period of time, and makes the actual transition crossing speed 50 times faster [10].

Although the $\gamma_t$-jump is essential for PS operation, it perturbs the optics during the transition crossing (1980 ms – 2080 ms). In order to characterise this perturbation, the $\beta$ functions were measured using k-modulation [11]. These measurements were conducted at the flat bottom energy of 2 GeV, while firing the $\gamma_t$-jump quadrupoles. This configuration was chosen to have better sensitivity of the k-modulation measurements for the available currents of the individual quadrupoles of the PS. The currents for the doublets and triplets of the $\gamma_t$-jump scheme were scaled accordingly, to reproduce the actual transition crossing optics.

As shown in Fig. 4, the measured $\beta_x$ values are in good agreement with the model predictions from MAD-X [12]. The perturbations during transition crossing are significant

ISBN: 978-3-95450-247-9 ISSN: 2673-5490 doi: 10.18429/JACoW-IPAC2024-THPC15

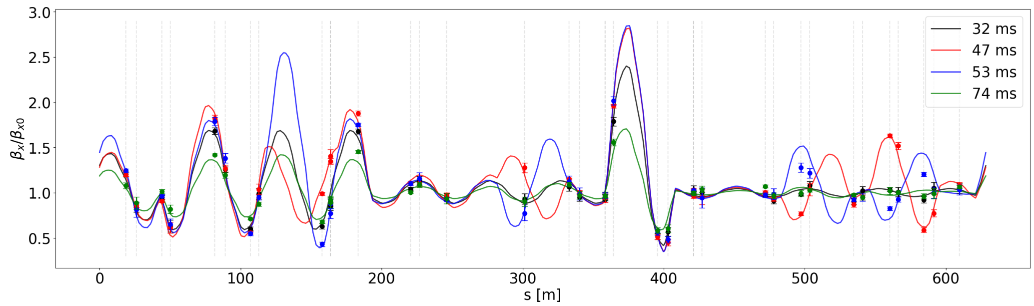


Figure 4: Horizontal $\beta$-beating resulting from the $\gamma_t$-jump scheme. The model (continuous lines) display the beta beating along the whole machine and the measured values (points with error-bars) verify it at the measurement locations. The displayed times correspond to timestamps of the $\gamma_t$-jump $(0-100\text{ ms})$ with the transition crossing happening at 50 ms.

with a $\beta$-beating up to $\beta_x/\beta_{x0} \approx 2.8$ compared to the unperturbed optics. In addition to the $\beta$-beating, the $\gamma_t$-jump introduces a dispersion variation up to $D_x/D_{x0} \approx 2.4$ and tune variation of $Q_x = +0.023$ and $Q_y = +0.002$ in the horizontal and vertical planes respectively.

## PS GAMMA JUMP SIMULATIONS

Simulations of the $\gamma_t$-jump optics perturbations have been performed using the PS MAD-X model in Xsuite [13]. As a first stage the $\gamma_t$-jump elements, i.e. the quadrupole doublets and triplets, are powered at constant energy similar to the configuration used during the optics measurements. The quadrupoles' currents as well as the simulated emittance evolution during this optics manipulation are shown in Fig 5. It is shown that the optics manipulations alone (without collective effects) have no impact on the emittances.

As a next step, space charge was also included in the simulations. The space charge effect is particularly strong in the PS [14], as the induced maximum tune shift can reach $Q_{x,y} \approx -0.3$ for the high brightness beams. In addition, the measurements presented above have shown a dependency of the non-Gaussian tail population on the beam brightness. Although the space charge force reduces with energy, it is

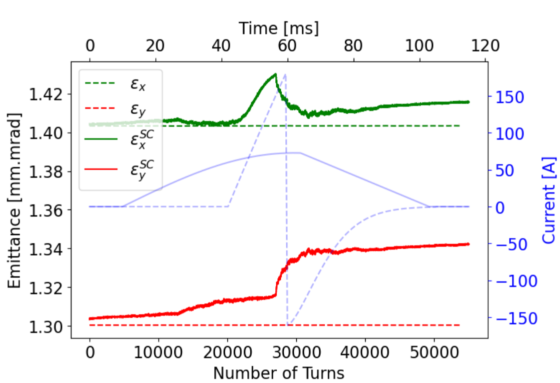


Figure 5: Vertical (red) and Horizontal (green) emittance along the $\gamma_t$-jump on a flat bottom cycle with (continuous) and without (dashed) space charge effects. The currents applied (blue) in the triplet (continuous) and doublet (dashed) quadrupoles are plotted on a secondary axis.

still significant around transition crossing. In particular, the maximum induced tune shift right before transition crossing was estimated from the measured beam characteristics as $Q_x = -0.06$ and $Q_y = -0.16$ [15]. As an initial simulation setup, in order to have a clearer view of the resonances affecting the beam during the $\gamma_t$-jump, a smaller tune spread of $Q_x = -0.05$ and $Q_y = -0.08$ was selected, which remains comparable to the measured values. As shown in Fig. 5, space charge affects the behaviour and an increase of the statistical rms emittance is observed in the horizontal plane during the first half of the $\gamma_t$-jump. In the second half of the $\gamma_t$-jump, this emittance increase is transferred to the vertical plane most likely due to interaction with the coupling resonance, which is excited by space charge (Montague resonance) [16–19], as the tunes evolve during the optics manipulation. Further simulation studies are needed, with different beam configurations, for a better characterisation of this phenomenon.

## CONCLUSION

The brightness curve was measured in the CERN PS at injection and extraction. The measurements show that the PS brightness is in good agreement with the LIU expectations. However, a significant increase of non-Gaussian transverse tail population was observed, with the transition crossing process identified as the main contributor. In addition, a dependence of the tail increase on beam brightness was identified. To this end, the optics perturbations along the $\gamma_t$-jump manipulations were measured at flat bottom energy and compared with the model showing excellent agreement. Finally, simulations of the $\gamma_t$-jump optics manipulation at constant energy are ongoing and have already shown an impact of space charge on the emittance evolution. Simulations also including acceleration are needed to fully characterize the mechanism causing the tail generation during transition crossing.

## ACKNOWLEDGEMENTS

The authors would like to thank the PSB and PS Operations, the equipment groups, J. Eldred, H. Rafique and F. Schmidt for their support on the measurements.

ISBN: 978-3-95450-247-9 ISSN: 2673-5490 doi: 10.18429/JACoW-IPAC2024-THPC15

# REFERENCES


[1] F. Asvesta *et al.*, "Characterization of transverse profiles along the LHC injector chain at CERN", in *Proc. IPAC'23*, Venice, Italy, May 2023, pp.WEPL158.
doi:10.18429/JACoW-IPAC2023-WEPL158

[2] S. Papadopoulou *et al.*, "Impact of non-Gaussian beam profiles in the performance of hadron colliders", in *Phys. Rev. Accel. Beams 23 10*, Oct. 2020 pp. 101004.
doi:10.1103/PhysRevAccelBeams.23.101004

[3] T. Prebibaj *et al.*, "Characterization of the Vertical Beam Tails in the CERN PS Booster", in *Proc. IPAC'22*, Bangkok, Thailand, Jun. 2022, pp. 218–221.
doi:10.18429/JACoW-IPAC2022-MOPOST057

[4] E. Métral and D. Möhl, "Transition Crossing", Technical Report, CERN-2011- 004, June 2011, pp. 59.

[5] H. Damerau, S. Hancock, A. Lasheen, and D. Perrelet, "RF Manipulations for Special LHC-Type Beams in the CERN PS", in *Proc. IPAC'18*, Vancouver, Canada, Apr.-May 2018, pp. 1971–1974.
doi:10.18429/JACoW-IPAC2018-WEPAF063

[6] S. Di Carlo *et al.*, "Commissioning of the LHC Injectors Upgrade fast wire scanners and first experimental results", *Nucl. Instrum. Methods Phys. Res.*, vol 1053, p. 168328.
doi:10.1016/j.nima.2023.168328

[7] F. Antoniou *et al.*, "Transverse Emittance Studies at Extraction of the CERN PS Booster", in *Proc. IPAC'19*, Melbourne, Australia, May 2019, pp. 1058–1061.
doi:10.18429/JACoW-IPAC2019-MOPTS087

[8] W. Van Goethem *et al.*, "Zero Dispersion Optics to Improve Horizontal Emittance Measurements at the CERN Proton Synchrotron", in *Proc. IPAC'22*, Bangkok, Thailand, Jun. 2022, pp. 503–506.
doi:10.18429/JACoW-IPAC2022-MOPOTK028

[9] H. Damerau *et al.*, "LHC Injectors Upgrade, Technical Design Report, Vol. I: Protons", Technical Report, CERN-ACC-2014-0337, Dec 2014.

[10] W. Hardt, "Gamma-transition-jump scheme of the CPS", in *Ninth international conference on high energy accelerators*, Stanford, 2-7 May 1974, CONF 740522, p. 434-438.

[11] T. Prebibaj *et al.*, "Injection Chicane Beta-Beating Correction for Enhancing the Brightness of the CERN PSB Beams", in *Proc. HB2021*, 2022, pp. 112-117.
doi:10.18429/JACoW-HB2021-MOP18

[12] L. Deniau, E. Forest, H. Grote and F. Schmidt, computer code MAD-X, http://madx.web.cern.ch/madx/.

[13] G. Iadarola *et al.*, "Xsuite: a flexible python toolkit for beam dynamics", presented at IPAC'24, Nashville, Tennessee, USA, May 2024, paper 2055, this conference.

[14] F. Asvesta *et al.*, "Identification and characterization of high order incoherent space charge driven structure resonances in the CERN Proton Synchrotron", Phys. Rev. Accel. Beams 23, 091001, 2020.
doi:10.1103/PhysRevAccelBeams.23.091001

[15] F. Asvesta and H. Bartosik, "Resonance Driving Terms From Space Charge Potential", CERN, Geneva, Switzerland, CERN-ACC-NOTE-2019-0046, Oct. 2019.
https://cds.cern.ch/record/2696190.

[16] B. W. Montague, "Fourth-Order Coupling Resonance Excited by Space Charge Forces in a Synchrotron", CERN-Report No. 68-38, CERN, 1968.

[17] I. Hofmann, G. Franchetti, J. Qiang, and R. D. Ryne, "Dynamical Effects of the Montague Resonance", in *Proc. EPAC'04*, Lucerne, Switzerland, Jul. 2004, paper WEPLT053, pp. 1960–1962.

[18] E. Métral *et al.*, "Intensity Dependent Emittance Transfer Studies at the CERN Proton Synchrotron", in *Proc. EPAC'04*, Lucerne, Switzerland, Jul. 2004, paper WEPLT029, pp. 1894–1896.

[19] F. Asvesta, "Space charge and lattice driven resonances at the CERN injectors", Ph.D. thesis, National Technical University of Athens, 2020.